J|A|C|S
ARTICLES
Published on Web 09/18/2004

Catalytic Unfolding and Proteolysis of Cytochrome *c* Induced by Synthetic Binding Agents

Kevin Groves, Andrew J. Wilson, and Andrew D. Hamilton*

Contribution from the Department of Chemistry, Yale University, New Haven, Connecticut 06511

Received December 17, 2003; E-mail: andrew.hamilton@yale.edu

Abstract: A class of polyanionic copper porphyrin dimers is shown to selectively increase the susceptibility of cytochrome *c* to proteolysis through binding-induced disruption of tertiary and secondary structure. The free energy of the protein conformation leading to proteolytic attack is stabilized by about 2.4 kcal/mol in the bound state. The proteolytic acceleration is catalytic in nature, requiring only a fraction of an equivalent of metalloporphyrin to effect complete, rapid digestion in the presence of a protease.[1]

Introduction

The binding of synthetic agents to large areas on a protein surface represents a relatively new approach to protein recognition and enzyme inhibition. In contrast to active site inhibitors, such allosteric receptors do not target the active site of the protein directly, but rather a large number of different functional groups for selective binding interactions.[2−4]

But beyond surface recognition of native protein conformations, there lies the potential for recognition of non-native conformations that are induced by a binding event.[5,6] Binding-induced conformational changes or even significant unfolding of an active protein with subsequent loss of function represents an emerging strategy for the modulation of protein function.[7,8] Recently, we have reported a family of substituted porphyrin derivatives that strongly bind to and induce unfolding of cytochrome *c* (cyt. *c*), selectively and stoichiometrically below room temperature and under nearly physiological conditions (pH 7.4, 50 mM NaCl).[6,9,10]

In addition to the disruption of protein function, protein unfolding plays a key role in the process of protein disposal through proteolytic digestion. Proteolysis requires conformational mobility of segments of a protein in order for the peptide bonds to reach the active site of a protease for cleavage.[11−15] In their native folded forms, many proteins are resistant to proteolytic degradation because stable secondary and tertiary structures effectively shield the peptide backbone from the protease. In such cases, the folded structure must be disrupted in order for efficient proteolysis to occur. In the laboratory, this can be accomplished by the use of relatively high concentrations of chemical denaturants or high temperatures.[13] However, denaturation by such drastic measures is inherently nonselective. In Nature, selective degradation of proteins is accomplished under physiological conditions. As an example, in the natural proteolytic degradation system of ClpA/ClpP, part of the Clp/Hsp100 family, tagged proteins are first selectively unfolded by ClpA through an ATP dependent denaturation step prior to being fed into a proteolytic chamber of ClpP for degradation.[1]

Selective degradation of target proteins by synthetic agents is an attractive goal, but one that has been difficult to achieve.[16,17] Targeted protein degradation offers the possibility of catalytic antagonists that could deactivate numerous equivalents of the target enzyme. Davis et al. have demonstrated selective and catalytic protein degradation by covalently attaching active site binders of targeted proteins to a protease.[17] In their system, the binding group recognizes the target protein, bringing the protease into close vicinity for proteolytic attack. Much earlier, Wilchek et al. attempted to use biotinylated proteases to enhance the proteolysis of avidin and streptavidin, biotin binding proteins that show high thermodynamic stability and resistance to proteolytic degradation.[16] However, the activity of the biotinylated proteases was inhibited by complexation with avidin. Thus, simply bringing a protease into close proximity with a protein by means of a binding group does not guarantee

(1) Weber-Ban, E. U.; Reld, B. G.; Miranker, A. D.; Horwich, A. L. *Nature (London)* **1999**, *401*, 90−93.
(2) Jain, R. K.; Hamilton, A. D. *Org. Lett.* **2000**, *2*, 1721−1723.
(3) Peczuh, M. W.; Hamilton, A. D. *Chem. Rev.* **2000**, *100*, 2479−2493.
(4) Park, H. S.; Lin, Q.; Hamilton, A. D. *J. Am. Chem. Soc.* **1999**, *121*, 1, 8−13.
(5) Shi, L.; Palleros, D. R.; Fink, A. L. *Biochemistry* **1994**, *33*, 7536−7546.
(6) Jain, R. K.; Hamilton, A. D. *Angew. Chem., Int. Ed.* **2002**, *41*, 641−643.
(7) Peterson, J. R.; Lokey, R. S.; Mitchison, T. J.; Kirschner, M. W. *Proc. Natl. Acad. Sci. U.S.A.* **2001**, *98*, 10 624−10 629.
(8) Leung, D. K.; Yang, Z.; Breslow, R. *Proc. Natl. Acad. Sci. U.S.A.* **2000**, *97*, 5050−5053.
(9) Wilson, A. J.; Groves, K.; Jain, R. K.; Park, H. S.; Hamilton, A. D. *J. Am. Chem. Soc.* **2003**, *125*, 4420−4421.
(10) Aya, T.; Hamilton, A. D. *Bioorg. Med. Chem. Lett.* **2003**, *13*, 2651−2654.
(11) Fontana, A.; Fassina, G.; Vita, C.; Dalzoppo, D.; Zamai, M.; Zambonin, M. *Biochemistry* **1986**, *25*, 1847−1851.
(12) Hubbard, S. J.; Eisenmenger, F.; Thornton, J. M. *Protein Sci.* **1994**, *3*, 757−768.
(13) Bark, S. J.; Muster, N.; Yates, J. R. I.; Siuzdak, G. *J. Am. Chem. Soc.* **2001**, *123*, 1774−1775.
(14) Hu, Y.; Fenwick, C.; English, A. M. *Inorg. Chim. Acta* **1996**, *242*, 261−269.
(15) Wang, L.; Chen, R. X.; Kallenbach, N. R. *Proteins: Struct., Funct., Genet.* **1998**, *30*, 435−441.
(16) Bayer, E. A.; Grootjans, J.; Alon, R.; Wilchek, M. *Biochemistry* **1990**, *29*, 11 274−11 279.
(17) Davis, B. G.; Sala, R. F.; Hodgson, D. R. W.; Ullman, A.; Khumtaveeporn, K.; Estell, D. A.; Sanford, K.; Bott, R. R.; Jones, J. B. *ChemBioChem* **2003**, *4*, 533−537.

that a favorable conformation for proteolytic attack can easily be reached. We describe here a multicomponent catalytic system for the rapid, efficient and catalytic digestion of cyt. *c* that involves conformational activation through selective binding and unfolding of the protein by substituted metalloporphyrins. The porphyrins target proteolytically resistant α-helical structures for unfolding, allowing facile proteolysis by trypsin or other proteases that leads to release of the activating binder back into solution to continue a catalytic cycle.

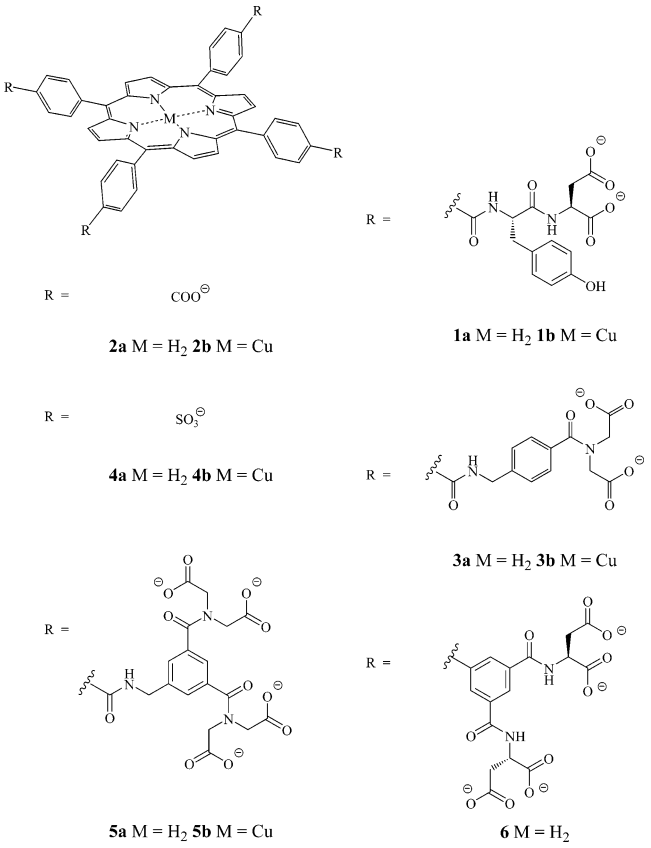

Results and Discussion

One of our first generation of protein binding porphyrins, **1a**, substituted with four tyrosine−aspartic acid dipeptides, binds to natively folded cyt. *c* as a 1:1 complex with a dissociation constant of 20 nM.[2] The simple derivative **2a**, first reported to bind to cyt. *c* by Fisher,[18] binds more weakly (K_d = 950 nM) and has only a very small effect on the thermal stability of cyt. *c*. In contrast, free base porphyrin **1a** was found to lower the melting point of cyt. *c* by about 20 °C at a mole ratio of 1.2:1, and even further at higher equivalents.[6] Similar behavior to **1a** was found with achiral free base porphyrin **3a**, indicating that the precise configuration of hydrophobic and charged residues is not crucial for unfolding activity.[9] The melting transitions of cyt. *c* with 1.2 equivalents of **1a** or **3a** were found to be considerably broader than that of native cyt. *c*, suggesting that a second or third equivalent of the porphyrin may be binding to the unfolded protein, stabilizing it relative to the 1:1 complex with the native form. To investigate the stoichiometry of binding to unfolded cyt. *c*, the thermal melting behavior over a concentration range of porphyrin was monitored by CD at two

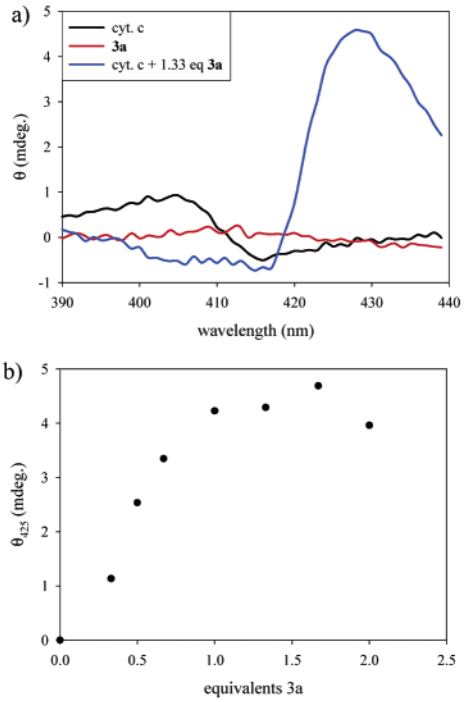

Figure 1. (a) CD spectra of cyt. *c* (black), **3a** (red) and their 1:1 complex (blue). (b) Titration of induced CD signal at 425 nm versus equivalents of **3a**.

wavelengths, 222 nm corresponding to the secondary structure of cyt. *c*, and at 425 nm, which represents an induced CD (presumably a coupling between the heme and the porphyrin) that is present in the 1:1 complex of folded cyt. *c* with **3a**, but which vanishes upon thermal unfolding (Figure 1).

With less than two equivalents of **3a** complete loss (corresponding to a final state equivalent to that at > 90 °C) of the induced CD signal centered at 425 nm occurred at a lower temperature than complete thermal denaturation of the protein secondary structure, as judged by the CD signal at 222 nm. Furthermore, the fraction of protein that was unfolded at the completion of the loss of induced CD was approximately half an equivalent relative to **3a** (Figure 2). However, when two or more equivalents of **3a** were present, the melting transitions observed for the two wavelengths coincided (Figure 3). These results indicate that there is a change in stoichiometry upon denaturation of the protein from a 1:1 complex with the native form to a 2:1 complex with the denatured state. With 1.2 equivalents of **3a**, only 60% of the protein can exist as a denatured 2:1 complex. The balance of protein remains in its native folded state, but uncomplexed.

At just below 85 °C (T_m of cyt. *c*), a single equivalent of **3a** can unfold the protein, while at lower temperatures (60−70 °C) and less than 1 equivalent of **3a** a disproportionation of the 1:1 complex with the native form into uncomplexed native protein and doubly bound unfolded protein occurs. Such disproportionation points to a cooperative role between the two binding events of **3a** to the denatured state that effects unfolding of cyt. *c* below its T_m. The change in stoichiometry also explains the increase in ΔT_m with increased **3a**, since higher concentrations will favor the doubly bound complex with the denatured state over the singly bound complex with the native conformation. The cooperativity of the transition can clearly be seen by plotting the fraction of unfolded cyt. *c* versus equivalents of **3a** at 60

(18) Clark-Ferris, K. K.; Fisher, J. *J. Am. Chem. Soc.* **1985**, *107*, 5007−5008.

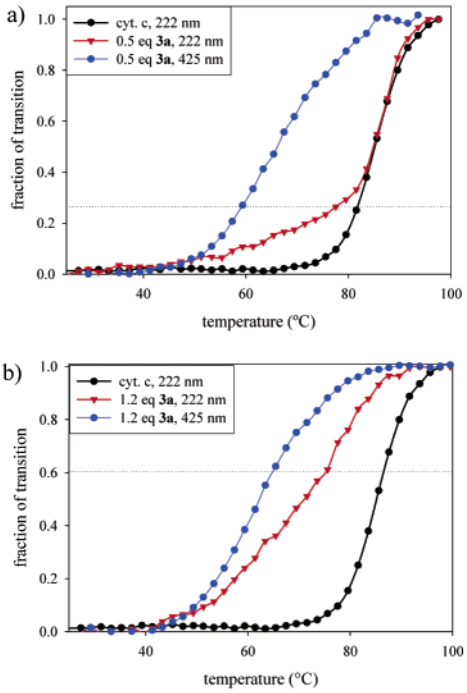

Figure 2. Thermal unfolding by CD of cyt. *c* at 222 nm (black), cyt. *c* + **3a** at 222 nm (red) and cyt. *c* + **3a** at 425 nm (blue) with (a) 0.5 equiv. **3a** and (b) 1.2 equiv. **3a**. Approximately half an equivalent of protein relative to **3a** is unfolded (red curve) at the temperature corresponding to complete loss of the 1:1 complex (blue curve).

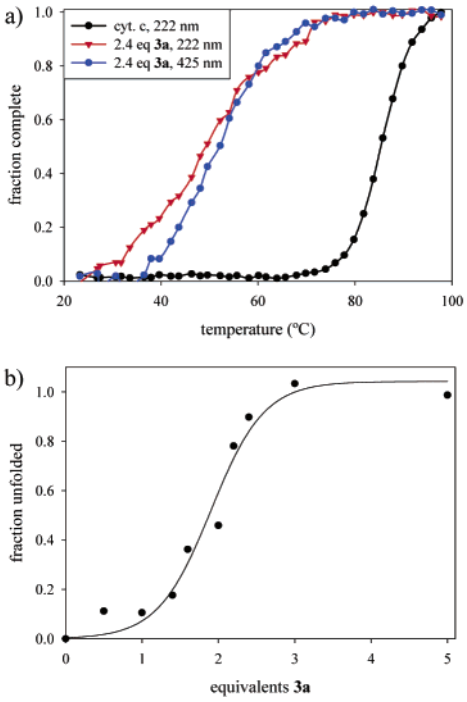

Figure 3. (a) Thermal unfolding by CD of cyt. *c* at 222 nm (black), cyt. *c* + 2.4 equiv. **3a** at 222 nm (red) and cyt. *c* + 2.4 equiv. **3a** at 425 nm (blue). (b) Titration of unfolding cyt. *c* by CD at 222 nm versus equivalents of **3a** at 60 °C.

°C, which shows a characteristic shape of a cooperative transition (Figure 3b).

Effects of Copper and RT Denaturation. Consistent with the observation of a preference for 2:1 binding to unfolded cyt. *c*, we have reported that the copper complexes of **1a** and **3a**, **1b** and **3b**, which exist largely as preformed dimers,[9,19,20] form

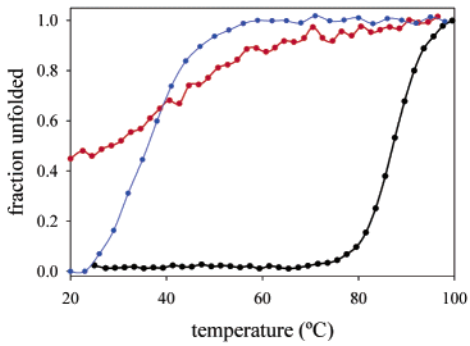

Figure 4. Thermal unfolding by CD of cyt. *c* at 222 nm (black), cyt. *c* 2.4 equiv. **3b** at 222 nm (red) and cyt. *c* + 2.4 equiv. **3b** at 410 nm (blue).

only 2:1 complexes with cyt. *c* and partially or fully unfold the protein below room temperature. The greater unfolding ability of the copper porphyrin dimers may result in part from the less favorable binding to the natively folded form, which would require breaking up of the dimer in order to form a preferred 1:1 complex observed with the free base porphyrins. Instead, the copper complexes unfold the protein even at low temperatures to allow 2:1 binding to the preformed dimer. Compound **1b** unfolds cyt. *c* essentially completely at room temperature, showing a CD spectrum that resembles the thermally unfolded protein (T > 90 °C).[9] For cyt. c bound by dimeric **3b**, two distinct conformational transitions are observed.

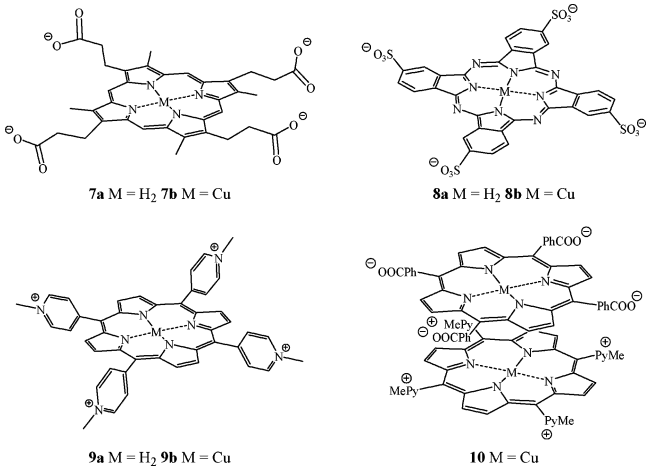

In addition to the loss of α-helical structure observed in the CD spectrum at 222 nm on addition of **3b**, the native coordination of methionine 80 to the heme is lost. A second transition, with a melting point of about 35 °C is also observed, and is characterized by further loss of α-helical character as determined by the CD signal at 222 nm as well as a distinct transition observable at 410 nm (Figure 4). The loss of the Met80 heme coordination is observable in the UV at 695 nm.[21] Heme coordination is lost upon 2:1 binding of copper complex **3b** at room temperature, observable by the band at 695 nm in the difference spectrum, but not upon 1:1 binding of free base **3a**, even in the presence of 2.2 equiv, further supporting the

(19) Pasternack, R. F.; Francesconi, L.; Raff, D.; Spiro, E. *Inorg. Chem.* **1973**, *12*, 2606−2611.
(20) Pasternack, R. F.; Huber, P. R.; Boyd, P.; Engasser, G.; Francesconi, L.; Gibbs, E.; Fasella, P.; Cerio Venturo, G.; Hinds, L. d. *J. Am. Chem. Soc.* **1972**, *94*, 4511−4517.
(21) Schejter, A.; Luntz, T. L.; Koshy, T. I.; Margoliash, E. *Biochemistry* **1992**, *31*, 8336−8343.

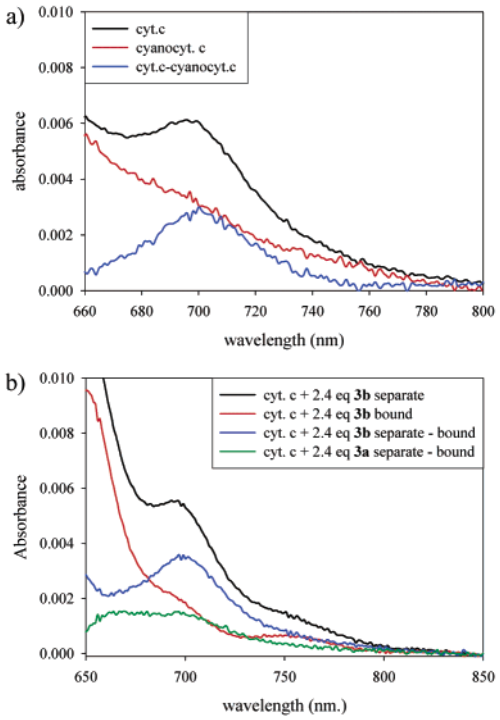

Figure 5. UV spectra of (a) cyt. *c* (black), cyanocyt. *c* (red), and cyt. *c*−cyanocyt. *c* (blue) and (b) cyt. *c* + 2 equiv. **3b** in separate tandem cells (black), cyt. *c* + 2.4 equiv. **3b** bound (red) their difference spectrum (separate−bound) (blue) and the corresponding difference spectrum for **3a** (green).

preference of 2:1 binding to unfolded forms of cyt. *c* in contrast to 1:1 binding to the native protein (Figure 5).

The disruption of the Met80 heme coordination is not critical for stability of the α-helical structure of cyt. *c*, however, since the cyanide complex of cyt. *c*, cyano-cyt. *c*, has a melting point (observed by CD at 222 nm) slightly higher than that of native cyt. *c*. Furthermore, the binding of **3b** to cyanocyt. *c* is equally strong as that to native cyt. *c*, suggesting that the porphyrins do not stack face-to-face with the heme, but rather interact with other regions of the protein to interfere with the stability of the secondary structure. Carey et al. have shown that the helical character of cyt. *c* requires the presence of N-terminal and C-terminal peptide regions (but not a significant segment in the middle) and the heme, even noncovalently bound. Thus, the stability of the secondary structure of the C-terminal fragment of cyt. *c* depends on tertiary interactions, which can be disrupted by binding a porphyrin.

The denaturation activity of copper porphyrins **3b** and **1b** results from the preferential binding of two equivalents of the porphyrins to a denatured state of cyt. *c*. The substituents of the copper porphyrin dimers, in contrast to the free bases, are not essential to the denaturation effect. Rather, the substituents of the copper porphyrins act to increase the binding affinity, hence allowing denaturation to occur at lower concentrations. At concentrations above μM, dimeric[19] copper porphyrins **2b** and **4b** also effected considerable denaturation of cyt. *c* at room temperature, while the corresponding monomeric free base porphyrins **2a** and **4a** showed only modest melting point depressions of about 15 °C.

Tetraanionic coproporphyrin-I **7a**, which lacks meso phenyl groups and binds weakly to cyt. *c*, as well as its copper complex **7b** had no effect on the stability of the protein (Figure 6).

Phthalocyanine tetrasulfonate **8a** and its copper complex **8b** induced small but identical melting point depressions, whereas the cationic tetra(4-methylpyridinium)porphyrin **9a**, which shows no affinity for cyt. *c*, and its copper complex **9b** had no effect on the structure of cyt. *c*. Free copper ions lower the melting point of cyt. *c* by about 5 °C, but when complexed with 1,4,8,11-Tetraaza-cyclotetradecane (cyclam) show no effect, suggesting the small melting point decrease is related to nonspecific interaction of the free copper ions with various side chains that are buried in the native form and exposed upon thermal denaturation. Thus, porphyrin bound copper ions themselves do not appear to play a significant role in cyt. *c* denaturation outside of increasing the stacking propensity of the porphyrin surface.

To further investigate the role of charged copper tetraphenylporphyrin dimers, we looked at the activity of the heterodimer **10** between **2b** and **9b**,[22] which is water soluble but charge neutral. This heterodimer showed essentially no effect on the structure of cyt. *c*, reinforcing the necessity of negative charge to complement the positive charge on the protein. Indeed, complexation of **2b** with **9b** completely eliminated the activity of **2b**.

A dimeric porphyrin, or even two equivalents, is not always necessary to lower the melting point of cyt. *c*, however. Dimerization can be prevented by substituting the porphyrin with more negative charge, as in compound **5a** with 16 carboxylates which does not dimerize due to the electrostatic repulsion of the carboxylates. **5a** binds cyt. *c* very strongly (K_d = 4 nM) and induces a melting point depression of about 20 °C. The same melting point depression was observed with 1 or 2 equivalents of **5a** as well as with its copper complex **5b**, confirming 1:1 binding stoichiometry and further implicating the role of copper as a means of inducing dimerization and 2:1 binding in the cases of porphyrins with less negative charge. Similarly, compound **6**, also with 16 carboxylates but with additional hydrophobic surface, was reported to have an even greater effect on the structure of cyt. *c*, showing a melting point of about 35 °C.[10] The behavior of **6** was also cleanly 1:1, due again to the electrostatic repulsion of 16 carboxylates. But the effects of the dimers are not just to form an entity that has double the negative charge of the monomer. Not one of **5a**, **5b** or **6** unfolded cyt. *c* at room temperature like the copper tetraphenylporphyrin dimers, even those with only 4 carboxylates. Therefore it must be a critical aspect of the anionic tetraphenylporphyrin dimer that imparts the greatest denaturing effect on cyt. *c*.

It is important to note that strong binding of this class of compounds to cyt. *c*, although necessary for denaturation at low concentrations, is not a general predictor for denaturing activity. As an example, compound **5a**, which binds with 4 nM affinity, only induces a 20 °C melting point depression, whereas **6**,[10] with slightly better affinity, showed a 50 °C depression. This is because the molecules can bind to both the natively folded as well as any of a collection of various unfolded states. The stronger the binding to the natively folded form, the weaker any denaturation effect will be. Thus, it is selectivity for the denatured state over the native state that drives the denaturation process for a particular porphyrin. Charge matching can increase the general affinity of the receptor for the protein, but does not

(22) Erdem, S. S. *J. Porphyrins Phthalocyanines* **1998**, *2*, 61−68.

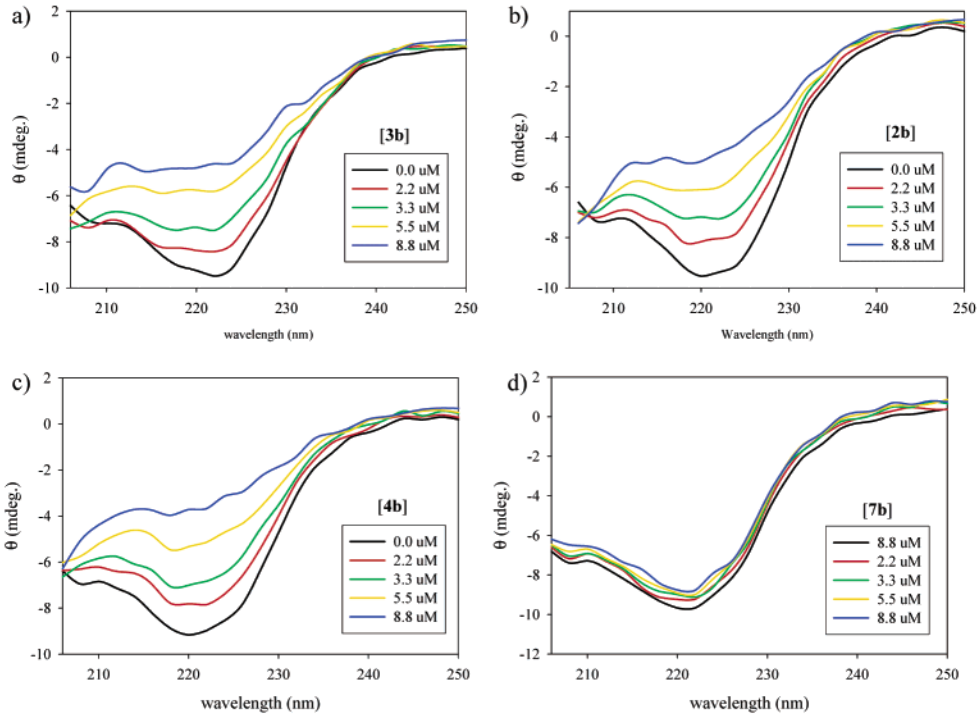

Figure 6. CD titration showing unfolding of cyt. c with 0 to 8.8 equivalents of (a) **3b**, (b) **2b**, (c) **4b**, and (d) **7b**.

necessarily translate into greater denaturing activity. The design of the next generation of targeted denaturants should focus on this difference, perhaps targeting disparate functionality on a folded protein that could better interact with a synthetic receptor in a less rigid unfolded state.

Catalytic Digestion of Cyt. *c*. Cytochrome *c* is a highly stable protein (T_m = 85 °C) that is relatively resistant to proteolysis. Even after 20 h in the presence of trypsin (0.02 μg/μL) at 21 °C and pH 7.4, minimal digestion was detectable by SDS-PAGE analysis. In contrast, with the addition of two equivalents of dimeric **3b** under the same conditions, the bulk of the protein was digested within 15 min and the digestion was essentially complete within 30 min (Figure 7). Furthermore, when the assisted digestions were complete, **3b** and trypsin remained active, since the digested fragments do not associate with the porphyrin. Thus, the system should be catalytic, as the porphyrin will be free to bind and activate additional protein after each digestion cycle.

Kinetic measurements of relative digestion rates were obtained by monitoring the CD signal at 222 nm, which reflects the degree of α-helical character of the folded protein in the sample, in a manner similar to that of Wang and Kallenbach.[23] The CD signal of cyt. *c* was unaffected by catalytic amounts of achiral **3b** under experimental conditions, and the signal from trypsin was negligible. MALDI−MS and SDS-PAGE analyses revealed that under the reaction conditions there was no significant accumulation of large peptide fragments during the course of the digestions. Instead, after the first cut was made on the protein, the remaining thermodynamically less stable pieces were digested to small peptide fragments quickly, thus allowing a continuous quantitative measure of the concentration of undigested cytochrome *c* during the course of the digestion by CD.

Using this method, 0.1 equivalents of dimeric **3b** resulted in complete digestion of cyt. *c* in the presence of trypsin in approximately 4 h at 30 °C and pH 7.4, whereas cyt. *c* and trypsin without **3b** resulted in less than 15% digestion in the same time. Just 0.025 equivalents of dimeric **3b** effected completion within 20 h, while the digest with trypsin alone had not even reached one-third completion in that time, representing more than 25 catalytic turnovers relative to dimeric **3b** (Figure 8).

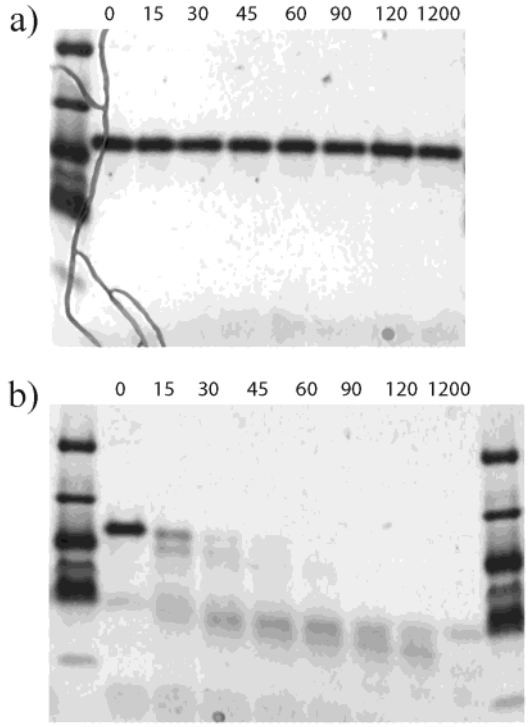

Figure 7. SDS-PAGE analysis of the tryptic digestion of cytochrome *c* (a) alone and (b) in the presence of 4 equiv. **3b**. Digestion time shown in minutes.

(23) Wang, L.; Kallenbach, N. R. *Protein Sci.* **1998**, *7*, 2460−2464.

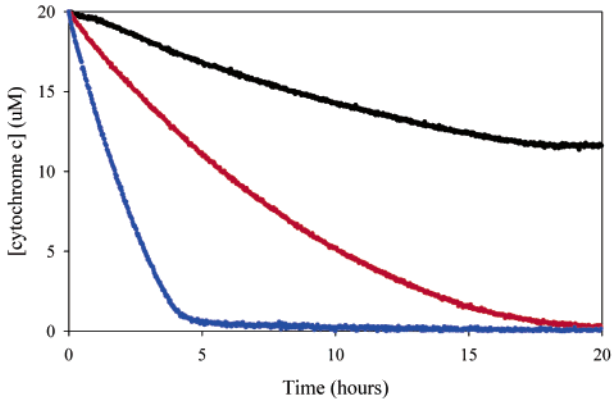

Figure 8. Kinetics of the tryptic proteolysis of cytochrome *c* (20 μM) as measured by CD at 222 nm, 30 °C, 5 mM sodium phosphate, 50 mM NaCl, 0.02 μg/μL trypsin with 0.0 (black), 0.025 (red), and 0.10 (blue) equivalents of dimeric **3b**.

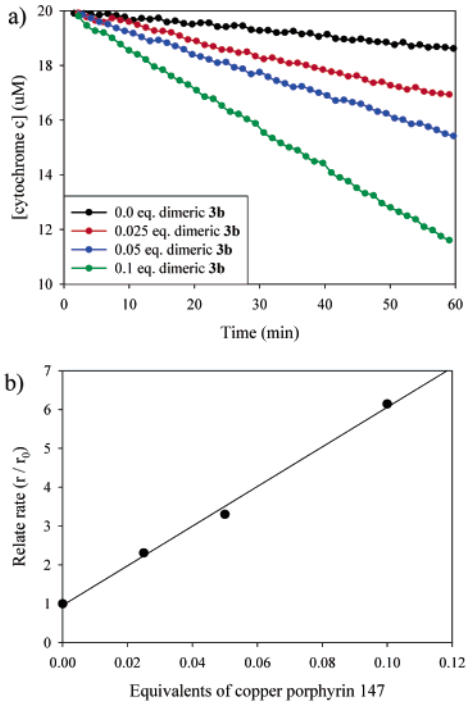

Figure 9. (a) initial rate kinetics for tryptic digestion of cyt. c with 0.0, 0.025, 0.05, and 0.1 equiv. of dimeric **3b** at 35 °C and (b) plot of relative rate of initial digestion versus catalytic equivalents of dimeric **3b**.

Under the same conditions, the benchmark hydrolysis of *N*-benzoyl arginine ethyl ester (BAEE) by trypsin was actually inhibited, proceeding at only 75% in the presence of 2 μM dimeric **3b**, presumably from weak binding of the porphyrin to trypsin. Figure 9a shows the initial rates of cyt. *c* digestion by trypsin with varying catalytic concentrations of **3b**. By plotting the initial rates of tryptic digestion with varying equivalents of dimeric **3b** (shown in Figure 9b) and extrapolating to 1 full equivalent, we found an acceleration of more than 50-fold for the tryptic digestion of the complex of cyt. *c* with dimeric **3b** over the native protein. Despite the fact that **3b** binds cyt. *c* as a 2:1 complex (by Job analysis),[9] the apparent kinetic order of **3b** in the catalyzed digestion was found to be 1. This result reflects that the porphyrins exist as dimers under the reaction conditions, so the reaction is effectively first order in dimer, but also that the concentrations of the protein and porphyrin

Table 1. Relative Initial Rates of Tryptic Digestion of Cyt. *c* in the Presence of Catalytic Amounts of Various Porphyrins

	initial rate (μM min^{-1})	relative initial rate[a]
cyt. *c*	0.023	1
cyanocyt. *c*	0.081	3.5
cyt. *c* + 0.05 equiv. **3b**	0.053	2.3
cyt. *c* + 0.10 equiv. **3b**	0.076	3.3
cyt. *c* + 0.20 equiv. **3b**	0.14	6.1
cyt. *c* + 0.20 equiv. **3a**	0.058	2.5
cyanocyt. *c* + 0.20 equiv. **3b**	0.44	19 (5.4[b])
cyt. *c* + 0.20 equiv. **5a**	0.030	1.3
cyt. *c* + 0.20 equiv. **2a**	0.035	1.5
cyt. *c* + 0.02 equiv. **2b**	0.15	6.5

[a] Rates were obtained by CD at 222 nm in 5 mM sodium phosphate, pH 7.4, 30 °C under initial rate conditions. [b] Rate relative to cyanocyt. *c*.

are high enough to ensure saturated 2:1 binding. Relative rates of proteolysis have been used previously to estimate free energy differences, relative to the conformation for proteolytic attack, between cyt. *c* in the oxidized and reduced forms as well as the azide complex.[23] The 50-fold acceleration for tryptic proteolysis observed for the complex of cytochrome *c* with **3b** at 30 °C corresponds to a lowering of the free energy necessary to reach the conformation(s) for initial proteolytic attack by ~2.4 kcal/mol.

Other cyt. *c* binders can also increase the susceptibility of the protein to proteolysis—heme ligands such as cyanide or azide, which disrupt native heme coordination of the protein by displacing Met80, also accelerate proteolysis.[14,23] Indeed, heme ligation of cyt. *c* has been shown to be critical for its resistance to proteolytic attack.[14] English et al. examined various metalloderivatives of cytochrome *c*, and correlated the strength of Met80 coordination with resistance to proteolysis. The coordination of Met80 must be broken in order for the protein to reach conformations for efficient peptide bond cleavage. The observed disruption of the native heme ligation of cyt. *c* by binding of **3b** likely contributes to the increase in susceptibility of cyt. *c* to trypsin.

Displacement of Met80 coordination cannot be the only effect contributing to the activation of cyt. *c* to digestion, however. The rate of proteolysis of the cyanide complex of cyt. *c* is still 25 times slower than that of the complex with **3b**. Furthermore, in the presence of 0.1 equivalents of dimeric **3b**, digestion of the cyanide complex was accelerated about the same amount as native cytochrome *c*, suggesting an alternative mechanism of action (Table 1). The disruption of the α-helical secondary structure, which is particularly resistant to proteolysis[11] and is observable by the thermal behaviors of the CD signal at 222 nm of the bound complex, contributes greatly to the marked rate enhancement of digestion.

To probe the specific regions of cyt. *c* that are made vulnerable to proteolytic attack in the presence of **3b**,[24] limited digestions were carried out and the results subjected to MALDI-TOF analysis. The peaks in the MALDI spectrum that correspond to initial cleavage fragments early in the digestion were identified, and locations of those cuts within the protein were determined. Sites of initial cleavage were determined only when

(24) With 2.2 equivalents the steady-state concentration of partially digested fragments is high enough to identify in the MALDI spectrum, whereas with catalytic amounts few large fragments are observed. For the digestion of cyt. *c* alone, higher concentrations (50 μM) were used to allow observation of low concentrations of intermediate fragments.

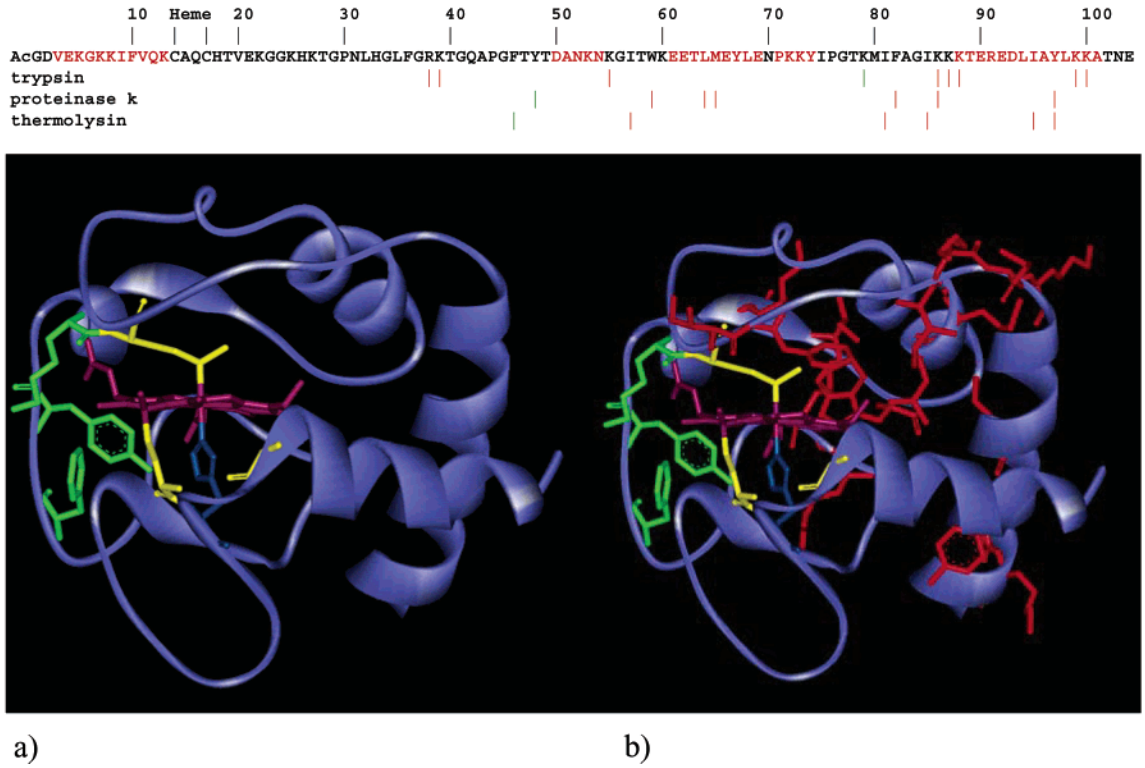

Figure 10. Location of unassisted (green) and **3b** assisted cleavage sites (red) for digestion of cytochrome *c* with trypsin, proteinase k, and thermolysin. α-Helical regions of the text sequence of the protein are shown in red.

both fragments of a single cut on the intact protein could be detected.

Three different proteases, trypsin, proteinase K and thermolysin, with varying residue selectivity and electrostatic properties were chosen. To observe the greatest increase in proteolytic sensitivity, digestions were carried out at 25 °C, below the optimal temperature for the proteases. Under these conditions, each protease shows significant initial digestion at only one location in the absence of any porphyrin, based on observable fragments. Although all three proteases cleave different residues, each cleavage site lies along loop regions in the same area of the protein around the heme crevice (Figure 10). This result is consistent with the observations by English[14] that the strength of heme ligation is a predictor of the rate of proteolysis.

In the presence of **3b**, however, fragments from a multitude of different initial cleavage sites were observed with all proteases over a fairly large distribution throughout the protein (Figure 10). The cleavage occurred irrespective of secondary structure along loop and α-helical regions (Glu61 through Glu69 and Lys88 through Ala101, red in Figure 10), but with a distinct preference for the C-terminal half of the protein. No initial cleavage was observed around the heme nor on the N-terminal α-helix (Val3 through Lys13). The general locations of assisted cleavages were consistent across the three different proteases, indicating that the effects are not specific to any one protease, but a result of the propterties of the porphyrin/cyt. *c* complex.

In order for a residue inside an α-helix to be cleaved, the helix must unwind so that the peptide bond can reach the active site of the protease. The presence of initial cuts within α-helices that do not occur in the absence of **3b** corroborates the CD evidence that the α-helical secondary structure of cytochrome *c* is being disrupted by the presence of the binders. Furthermore, the distribution of initial assisted cleavage sites indicates that the proteolytic acceleration is not a result of making just a single residue or region vulnerable, but a more general disruption in the stability of the secondary structure of the protein. Under saturation conditions, where concentrations of porphyrin are far above the binding constant, unsubstituted copper porphyrin **2b** induced cleavage at essentially the same locations as substituted compound **3b**, reaffirming the role of the copper porphyrin dimer core as the active component for denaturation.

As with denaturation effects, the acceleration of digestion of cytochrome *c* by the copper porphyrin dimers is selective. Cytochrome *c*551, which shares major structural features with cytochrome *c* but lacks much of the surface positive charge shows no proteolytic acceleration in the presence of **3b**. Myoglobin and α-lactalbumin were similarly unaffected by **1b**[9] and the tryptic hydrolysis of BAEE was actually slightly inhibited by **3b**, presumably through weak binding to trypsin, which also carries significant positive charge.

The porphyrins apparently do not function by relieving charge repulsion between a cationic protease (trypsin) and cationic substrate (cyt. *c*). Although 0.20 equivalents of essentially monomeric **3a** showed about 40% of the catalytic acceleration of tryptic digestion observed with **2b** or **3b**, hexadecacarboxylate **5a** had almost no effect on the rate of proteolysis, despite a low dissociation constant of 4 nM (Table 1). Additionally, initial rates of proteolysis by thermolysin and proteinase K, which carry less positive charge than trypsin, were accelerated to a similar extent by **3b** as found with trypsin. However, the accumulation of intermediate fragments precludes quantitative measurements of digestion rates of these proteases by CD spectroscopy. Thus, the nature and charge of the protease is not important to achieve accelerated digestion.

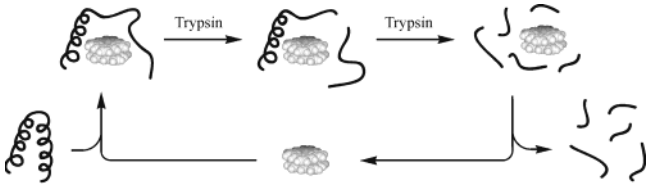

Figure 11. Proposed catalytic cycle for the accelerated digestion of cyt. *c* by a porphyrin dimer.

The copper porphyrins described here are conformational activators of the substrate protein that assist peptide bonds that are otherwise shielded inside α-helices or other folded structures in accessing the active site of a protease. The apparent catalytic activity toward digestion of cyt. *c*, depicted in Figure 11, arises from the recycling back into solution of the binder upon digestion of the bound protein. The kinetic acceleration for the digestion stems from the binding-induced unfolding of the protein, where all the necessary energy to effect denaturation is supplied in the form of excess binding energy. The catalytic cycle is driven forward entropically by the complete digestion of the protein and concomitant release of the binder back into solution.

Such a catalytic cycle, where synthetic porphyrins act as cocatalysts by conformationally activating a protein to cleavage by a protease represents a new strategy for directed protein degradation. Previously, a process of this type had only been seen in members of the proteasome family (such as ClpA/ClpP).[1] In the present case, the driving force for unfolding, rather than ATP, is the favorable thermodynamics of binding to the unfolded state of the protein.

Conclusions

In conclusion, we have demonstrated a selective and catalytic system for the efficient proteolytic digestion of cytochrome *c*. The effect is achieved by inducing substantial conformational changes, including disruption of native heme ligation and unraveling of α-helical secondary structure upon binding of synthetic porphyrin receptors to the protein. This results in a lowering of the free energy of the conformation for proteolytic attack by trypsin by ca. 2.4 kcal/mol, corresponding to more than 50-fold acceleration of proteolysis. We have observed up to 25 catalytic turnovers relative to the dimeric porphyrin entity. The sites of assisted cleavage are broadly distributed throughout the C-terminal half of the protein, indicating a general disruption of protein structure.

Experimental Section

General Details. Horse heart cytochrome *c*, proteinase K, thermolysin and cytochrome *c*551 were purchased from Sigma. Trypsin, modified, sequencing grade was purchased from Roche. Coproporphyrin-I, *meso* tetra-(4-carboxyphenyl)porphine and *meso* tetra-(4-sufonatophenyl) porphine were purchased from Strem. Phthalocyanine tetrasulfonate and *meso* tetra-(4-*N*-methylpyridinium) porphyrin were purchased from Calbiochem. Copper(II) phthalocyanine tetrasulfonate was purchased from Avocado. All other reagents were purchased from Aldrich and used without further purification. NMR spectra were obtained using a Brücker 400 DPX spectrometer. CD spectra were measured on an Aviv 62DS spectrapolarimeter. UV−vis spectra were measured using an Agilent A453 spectrometer. MALDI-MS spectra were recorded using an Applied Biosystems Voyager-DE Pro MALDI-TOF mass spectrometer. Fluorescence spectra were recorded using a Hitachi F-4500 fluorescence spectrophotometer. Horse heart cytochrome *c* was standardized spectrophotometrically using $\epsilon_{550} = 2.95 \times 10^4\ M^{-1}\ cm^{-1}$ after reduction with sodium dithionite (1 mg/mL) in 5 mM sodium phosphate, pH 7.4. Cyanocytochrome *c* was prepared by incubating cytochrome *c* (500 μM) in 5 mM sodium phosphate, pH 7.4 with 2 mM sodium cyanide at 37 °C for 30 min. Incorporation of cyanide was confirmed by loss of the band at 695 nm in the visible spectrum.[21] Stock solutions of proteins and porphyrins were prepared in 5 mM sodium phosphate buffer and the pH adjusted to 7.4. Protease solutions were prepared by dissolving the enzymes 1 μg/μL in 1.0 mM HCl and used fresh.

Proteolysis Experiments. For CD kinetic studies, 400 μL of 20 μM protein in 5 mM sodium phosphate buffer at pH 7.4 and various equivalents of porphyrins were equilibrated to the temperature of the reaction. Protease solution (4 to 8 μL of 1 μg/ μL protease) was added and the samples were vortexed for 15 s before being placed in the 2 mm quartz CD cells pre-equilibrated to the reaction temperature inside the CD sample holder. The CD signal at 222 nm was recorded with an averaging time of 15 s for 30 min to 20 h, depending on the rate of digestion.

For MALDI-TOF−MS analysis, 10 μL aliquots of digestion samples taken between 15 s and 30 min of addition of protease, depending on the rate of digestion, were quenched in 20 μL of a 10 mg/mL solution of sinapinic acid matrix in 50:50 H_2O/acetonitrile with 2% TFA. 0.5 to 1 μL of the quenched samples were spotted onto a 100 well stainless steel MALDI plate for analysis. Spectra were calibrated against the parent protein peak ($M+1 = 12361.2$). Sites of initial cleavage were determined by identification of both fragments that result from the cleavage.

For SDS-PAGE analyses, 60 μL of cytochrome *c* (20 μM) and porphyrin (80 μM) were incubated for 10 min. (5 mM phosphate, 50 mM NaCl, pH 7.4). Trypsin (2 μg in 2 μL of 0.1 N HCl) was added to the reaction mixture and at appropriate intervals, 10 μL of the solution was removed from the reaction mixture and quenched by addition to 20 μL tris sample buffer (Biorad 2%) and heating at 95 °C for 5 min. At the end of the reaction, the samples were loaded onto 16.5% tris/tricine gels and constant voltage of 100 V was applied for 2 h (running buffer 10x SDS tris/tricine). The gels were washed with water (15 min) 10% acetic acid 0.025% Commasie blue staining solution (2 h) and water (2 h). The gels were dried in the standard manner and imaged using a PC.

Syntheses. Stock solutions of tetra-(4-sufonatophenyl)porphine were standardized by UV using $\epsilon_{414} = 5.33 \times 10^5\ M^{-1}\ cm^{-1}$.[25] Stock solutions of coproporphyrin-I were standardized by UV using $\epsilon_{372} = 1.16 \times 10^5\ M^{-1}\ cm^{-1}$ for dimeric form at 200 mM NaCl.[26] Stock solutions of tetra-(4-*N*-methylpyridinium) porphyrin were standardized by UV using $\epsilon_{372} = 2.26 \times 10^5\ M^{-1}\ cm^{-1}$.[27]

Copper(II) Tetra-(4-carboxyphenyl) Porphine 2b. A 10-fold excess (w/w) of copper acetate was added to a solution of the free base tetra-(4-carboxyphenyl)porphine in methanol. After 12 h at room temperature, the insoluble copper porphyrin was then filtered off and washed with 1 mM HCl, distilled water, ethanol then ether and dried under vacuum. Incorporation of copper was confirmed by UV and stock solutions were standardized by UV using $\epsilon_{415} = 3.46 \times 10^5\ M^{-1}\ cm^{-1}$.[19]

Copper(II) Tetra-(4-sulfonatophenyl) Porphine 4b. A 10-fold excess of copper(II) acetate was added to a solution of the free base tetra-(4-sufonatophenyl) porphine in 95:5 methanol/water. After 12 h, the copper complex was precipitated with acetone and filtered. The filtrate was washed with acetone then washed off the filter with distilled water. Incorporation of copper was confirmed and stock solutions were standardized by UV using $\epsilon_{413} = 4.16 \times 10^5\ M^{-1}\ cm^{-1}$.[28]

(25) Larsen, R. W.; Omdal, D. H.; Jasuja, R.; Niu, S. L.; Jameson, D. M. *J. Phys. Chem. B* **1997**, *101*, 8012−8020.
(26) Giovannetti, R.; Bartocci, V.; Ferraro, S.; Gusteri, M.; Passamonti, P. *Talanta* **1995**, *42*, 1913−1918.
(27) Lu, M.; Guo, Q.; Pasternack, R. F.; Wink, D. J.; Seeman, N. C.; Kallenbach, N. R. *Biochemistry* **1990**, *29*, 1614−1624.

Copper(II) Coproporphyrin-I 7b. To a standardized aqueous stock solution of the free base coproporphyrin-I **7a** was added 1 equivalent of copper (II) acetate. Incorporation of copper was rapid requiring only about 5 min to reach completion as confirmed by UV−vis (5 mM phosphate, pH 7.4) λ 379, 530, 563 nm, which matches that reported in the literature.[26]

Copper(II) Tetra-(4-*N*-methylpyridinium) Porphyrin 9b. To a standardized aqueous stock solution of the free base tetra-(4-*N*-methylpyridinium) porphyrin **9a** was added 1 equiv of copper (II) acetate and the solution was allowed to stand at room-temperature overnight. Completion of metalation was confirmed by UV−vis (5 mM phosphate, pH 7.4) λ 425, 548 nm, which matches that reported in the literature.[22]

***meso*-Tetrakis-(4-carboxyphenyl-amidomethyl-benzoyl)-iminodiacetate) Porphyrin 3a.** To a vigorously stirred solution of 4-(aminomethyl)benzoic acid (1.0 g, 6.6 mmol) in 50 mL of water at 0 °C was added, slowly, benzylchloroformate (1.1 mL, 7.3 mmol) and the solution was warmed to room temperature and stirred for 16 h. The solution was acidified to pH 3 with 1 M HCl and the product filtered off as a pure white solid and washed with 50 mL each of water, ethanol and diethyl ether yielding 1.8 g (95%). The Z-protected 4-(aminomethyl) benzoic acid (260 mg, 0.91 mmol), di-*tert*-butyl-iminodiacetate (250 mg, 1.0 mmol) and 1-[3-(dimethylamino)propyl]-3-ethylcarbodiimide hydrochloride (EDC) (190 mg, 0.98 mmol) were placed in 25 mL of dry dichloromethane and stirred at room temperature for 4 h. The solution was extracted successively with 30 mL each of 1 M HCl, saturated sodium bicarbonate and brine, dried over sodium sulfate and evaporated to dryness. The product was purified on a silica column eluting with 2:1 hexanes/ethyl acetate yielding 375 mg (80%) of the Z-protected product as a white solid. The product (375 mg, 0.73 mmol) was deprotected by catalytic hydrogenation in 12 mL of vigorously stirred methanol with 10% Pd/C (42 mg, 0.04 mmol) catalyst under 1 atm of hydrogen for 4 h. The solution was filtered through Celite and the methanol was evaporated. The final product, di-*tert*-butyl-N−(4-aminomethyl-benzoyl)-iminodiacetate, was purified on a silica column eluting with dichloromethane with 0.5% triethylamine and an increasing fraction of methanol from 2.5% to 10% yielding the pure deprotected product as a colorless, sticky, solid (250 mg, 69% overall yield): ^{1}H NMR (400 MHz, $CDCl_3$) δ 7.39 (d, J = 8.1 Hz, 2H), 7.34 (d, J = 8.1 Hz, 2H), 4.16 (s, 2H), 3.95 (s, 2H), 3.90 (s, 2H), 1.47 (s, 9H), 1.44 (s, 9H).

To a solution of *meso*-tetrakis-(4-carboxyphenyl) porphyrin (63 mg, 0.08 mmol) in 10 mL of dry dichloromethane was added di-*tert*-butyl-*N*-(4-aminomethyl-benzoyl)-iminodiacetate (120 mg, 0.32 mmol) and 1-[3-(dimethylamino)propyl]-3-ethylcarbodiimide hydrochloride (EDC) (86 mg, 0.35 mmol), and the mixture was stirred at room temperature under nitrogen overnight. The reaction mixture was extracted successively with saturated sodium bicarbonate, 1 M sodium hydroxide and brine, dried over sodium sulfate and evaporated to dryness. The *tert*-butyl protected product was purified on a silica column eluting with dichloromethane with an increasing fraction of methanol from 0% to 5%. Treatment with 95% TFA/H_2O (5 mL) at room temperature for 4 h followed by evaporation afforded the triflate salt of the free acid product as a dark green solid (104 mg, 65%): ^{1}H NMR (400 MHz, DMSO-d_6) δ 9.40 (t, J = 5.0 Hz, 4H), 8.80 (s, 8H), 8.29 (d, J = 8.5 Hz, 8H), 8.26 (d, J = 8.5 Hz, 8H), 7.47 (d, J = 8.1 Hz, 8H), 7.29 (d, J = 8.1 Hz, 8H), 4.62 (d, J = 4.7 Hz, 8H) 4.08 (s, 8H), 3.97 (s, 8H), −3.00 (s, b, 2H); MALDI-TOF MS *m*/*e* 1783.5 $[M+H]^+$ calcd for $C_{96}H_{78}N_{12}O_{24}$(+H), found 1783.4; UV−vis (H_2O, 5 mM phosphate, pH = 7.4) λ 416, 517, 554, 581, 635 nm.

Copper(II) *meso*-Tetrakis-(4-carboxyphenyl amidomethyl-benzoyl)-iminodiacetate) Porphyrin 3b. Compound **3a** (15 mg, 0.0075 mmol) was dissolved in 5 mL of methanol and copper(II) chloride (2.5 mg, 0.019 mmol) was added. The solution was stirred for 3 h at room temperature, after which time a red precipitate had formed and all green color had vanished from the solution. The red solid was filtered and washed with methanol, 0.01 M HCl, and water. The solid was dissolved off the filter with DMF and evaporated to dryness yielding 12 mg of product (90%); MALDI-TOF−MS *m*/*e* 1844.5 $[M+H]^+$ calcd for $C_{96}H_{76}N_{12}O_{24}Cu$(+H), found 1844.4; UV−vis (H_2O, 5 mM phosphate, pH = 7.4) λ 416, 541, 576 nm.

***meso*-Tetrakis-[(4-carboxyphenylamidomethyl-isophthaloyl)-bis-iminodiacetate] Porphyrin 5a.** 5-[(Benzyloxycarbonyl)aminomethyl]isophthalic acid[29] (250 mg, 0.76 mmol), di-*tert*-butyl-iminodiacetate (465 mg, 1.9 mmol) and 1-[3-(dimethylamino)propyl]-3-ethylcarbodiimide hydrochloride (EDC) (306 mg, 1.6 mmol) were placed in 25 mL of dry dichloromethane and stirred at room temperature for 6 h. The solution was extracted successively with 30 mL each of 1 M HCl, saturated sodium bicarbonate and brine, dried over sodium sulfate, and evaporated to dryness. The product was purified on a silica column eluting with 1:1 hexanes/ethyl acetate yielding 375 mg (63%) of the Z-protected product as a white solid. The product (375 mg, 0.73 mmol) was deprotected by catalytic hydrogenation in 30 mL of vigorously stirred methanol with 10% Pd/C (25 mg, 0.023 mmol) catalyst under 1 atm of hydrogen for 24 h. The solution was filtered through diatomaceous earth and the methanol evaporated. The deprotected (aminomethyl-isophthaloyl)-bis-iminodiacetate tetra *tert*-butyl ester was purified on a silica column eluting with dichloromethane with 0.5% triethylamine and an increasing fraction of methanol from 2% to 5% yielding the pure deprotected product as a colorless, sticky, solid (265 mg, 88%): ^{1}H NMR (400 MHz, $CDCl_3$) δ = 1.43 (s, 18H), 1.47 (s, 18H), 3.85 (s, 2H), 3.91 (s, 4H), 4.16 (s, 4H) 7.32 (s, 1H), 7.46 (s, 2H).

To a stirred solution of meso-tetrakis-(4-carboxyphenyl) porphyrin (0.10 mg, 0.126 mmol) in anhydrous dichloromethane (25 mL) was added oxalyl chloride (390 uL, 4.4 mmol) and a catalytic amount of DMF (1μL). The reaction mixture was then stirred overnight under an inert atmosphere and dried for 8 h under high vacuum. The resultant acid chloride was then dissolved in 8 mL of freshly distilled tetrahydrofuran to which was added a solution of (aminomethyl-isophthaloyl)-bis-iminodiacetate tetra *tert*-butyl ester (0.27 g, 0.41 mmol) and diisopropylethylamine (0.7 mL, 4.1 mmol) in 10 mL of dichloromethane. The reaction mixture was allowed to stir under an inert atmosphere for 15 min then evaporated to dryness. The residue was dissolved in 40 mL of dichloromethane, washed successively with 10% citric acid, 1 M NaOH, and saturated NaCl, dried over sodium sulfate and evaporated to give 290 mg (98%) of crude product. The *tert*-butyl protected product was purified in small batches (~40 mg) on a column of Brockman grade III basic alumina eluting with dichloromethane with 1% methanol resulting in a yield of 92%. ^{1}HNMR (400 MHz, $CDCl_3$) δ = −2.87 (bs, 2H), 1.47 (s, 72H), 1.50 (s, 72H), 4.07 (s, 16H), 4.17 (s, 16H), 4.74 (bs, 8H), 7.20 (s, 4H), 7.60 (s, 8H), 8.40 (s, 16H), 8.91 (s, 8H), 9.56 (bs, 4H).

Treatment of the *tert*-butyl protected compound (35 mg, 0.011 mmol) with 95% TFA/H_2O (5 mL) at room temperature for 4h followed by evaporation afforded the triflate salt of the free acid **5a** as a dark green solid (28 mg, 100%). ^{1}HNMR (400 MHz, $CDCl_3$) δ = −2.93 (bs, 2H), 4.07 (s, 16H), 4.17 (s, 16H), 4.68 (s, 8H), 7.18 (s, 4H), 7.54 (s, 8H), 8.33 (s, 16H), 8.33 (s, 16H), 8.88 (s, 8H), 9.49 (bs, 4H). MALDI-TOF-MS *m*/*e* 2419.6 [M+H]+ calcd for $C_{116}H_{98}N_{16}O_{44}$(+H), found 2419.4. UV/vis (H_2O, 5 mM phosphate, pH = 7.4) λ 415, 518, 555, 581, 643 nm.

***meso*-Tetrakis-[(4-carboxyphenyl amidomethyl-isophthaloyl)-bis-iminodiacetate] Copper(II) Porphyrin 5b.** Compound **5a** (20 mg, 0.0076 mmol) was dissolved in 4 mL of methanol and copper(II) chloride (2.0 mg, 0.015 mmol) was added. The solution was stirred for 24 h at room temperature, after which time a red product was precipitated by addition of 15 mL of 0.1 M HCl. The red solid was

(28) Gibbs, E.; Skowronek, W. R., Jr.; Morgan, W. T.; Muller-Eberhard, U.; Pasternack, R. F. *J. Am. Chem. Soc.* **1980**, *102*, 3939−3944.

(29) Ritzen, A.; Frejd, T. *Eur. J. Org. Chem.* **2000**, 3771−3782.

filtered and washed with 0.01 M HCl and distilled water. The solid was then washed through the filter with methanol and evaporated to dryness yielding 16 mg of product (87%); MALDI-TOF−MS *m*/*e* 2480.5 [M+H]+ calcd for $C_{116}H_{96}CuN_{16}O_{44}$(+H), found 2480.4. UV/vis (H_2O, 5 mM phosphate, pH = 7.4) λ 414, 541 nm.

Acknowledgment. We thank the National Institutes of Health, Institute of General Medicine (GM35208) for financial support of this work.

JA0317731